

Contents

1	Numerical results for the Ising model	1
1.1	At the critical point	1
1.1.1	Existence of two length scales	1
1.1.2	Central charge	4
1.1.3	Using the entropy to define the correlation length . . .	5
1.1.4	Exponent κ	5
1.1.4.1	Comparison with exact result in asymptotic limit	7
1.2	Locating the critical point	7
1.2.1	Finite m	8
1.2.2	Finite N	10
1.3	Away from the critical point	10
1.4	Discussion	14
1.4.1	Finite- m vs finite-size simulations	14
1.4.2	Exponent κ	15
	Bibliography	16

1

Numerical results for the Ising model

We present numerical results of finite- m and finite-size scaling within the CTMRG method on the Ising model.

With finite- m simulations, it is much easier to reach large system sizes, but thermodynamic quantities do not grow smoothly as a function of m , as a result of the underlying spectrum of the corner transfer matrix. This makes it harder to fit the basic power law divergences. Defining the correlation length in terms of the classical analogue to the entanglement entropy mitigates this effect somewhat.

Quantities calculated with finite-size simulations do not suffer this unsmooth behaviour. Results for both methods are comparable, but it is plausible that finite-size data turns out to be more accurate when corrections to scaling are included.

Apart from thermodynamic quantities, we also accurately compute the central charge of the critical point with both methods. Additionally, we verify the relation $\xi(m) \propto m^\kappa$ at the critical point, although the value of κ found in this work is slightly lower than predicted in the literature.

1.1 At the critical point

1.1.1 Existence of two length scales

First, we reproduce the results presented in [1] to validate the assumption that at the critical point, the only relevant length scales are the system size N and the length scale associated to a finite dimension m of the corner transfer matrix $\xi(m)$. Here, we assume that $\xi(m)$ is given by the correlation length at the critical point, see ??.

The order parameter¹ should obey the following scaling relation at the

¹It is worth stressing that the order parameter and the magnetization per site are used inter-

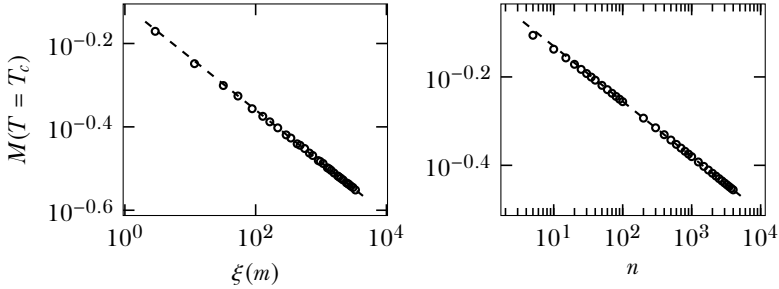


Figure 1.1: Left panel: fit to the relation in Eq. 1.1, yielding $\frac{\beta}{\nu} \approx 0.125(5)$. The data points are obtained from simulations with $m = 2, 4, \dots, 64$. The smallest 10 values of m have not been used for fitting, to diminish correction terms to the basic scaling law. Right panel: fit to conventional finite-size scaling law given in Eq. 1.2, fitted with $n = 1500, 1750, \dots, 4000$, calculated with a truncation error no larger than 10^{-7} , yielding $\beta/\nu \approx 0.1249$.

critical temperature

$$M(T = T_c, m) \propto \xi(T = T_c, m)^{-\beta/\nu}. \quad (1.1)$$

The left panel of Fig. 1.1 shows that this scaling relation holds. The fit yields $\frac{\beta}{\nu} \approx 0.125(5)$, close to the true value of $\frac{1}{8}$.

The right panel shows the conventional finite-size scaling relation

$$M(T = T_c, N) \propto N^{-\beta/\nu}, \quad (1.2)$$

yielding $\beta/\nu \approx 0.1249(1)$.

The correlation length $\xi(m)$ shows characteristic half-moon patterns on a log-log scale, stemming from the smeared-out stepwise pattern in the corner transfer matrix spectrum (see ??). This makes the data harder to interpret, since the effect of increasing m depends on how much of the spectrum is currently retained.

changeably for the Ising model, and that the magnetization per site is approximated, within the CTMRG algorithm, by the expectation value of the central spin. See ??.

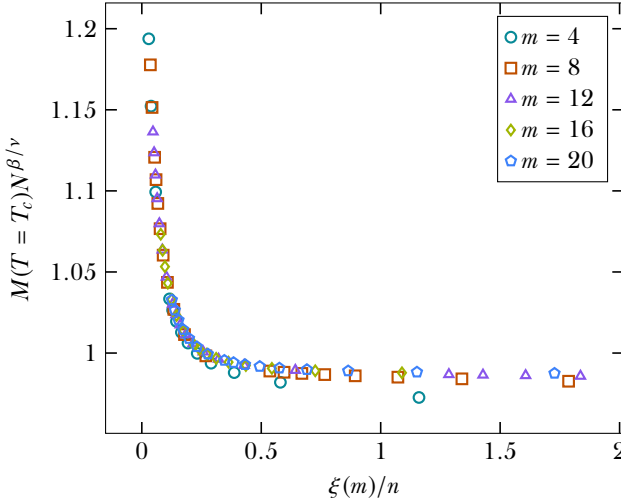


Figure 1.2: Scaling function $\mathcal{G}(\xi(m)/N)$ given in Eq. 1.3.

To further test the hypothesis that N and $\xi(m)$ are the only relevant length scales, the authors of [1] propose a scaling relation for the order parameter M at the critical temperature of the form

$$M(N, m) = N^{-\beta/\nu} \mathcal{G}(\xi(m)/N) \quad (1.3)$$

with

$$\mathcal{G}(x) = \begin{cases} \text{const} & \text{if } x \rightarrow \infty, \\ x^{-\beta/\nu} & \text{if } x \rightarrow 0, \end{cases} \quad (1.4)$$

meaning that Eq. 1.3 reduces to Eq. 1.2 in the limit $\xi(m) \gg N$ and to Eq. 1.1 in the limit $N \gg \xi(m)$. Fig. 1.2 shows that the scaling relation of Eq. 1.3 is justified.

Fig. 1.3 shows the cross-over behaviour from the N -limiting regime, where $M(N, m) \propto N^{-\beta/\nu}$ to the $\xi(m)$ -limiting regime, where $M(N, m)$ does not depend on N .

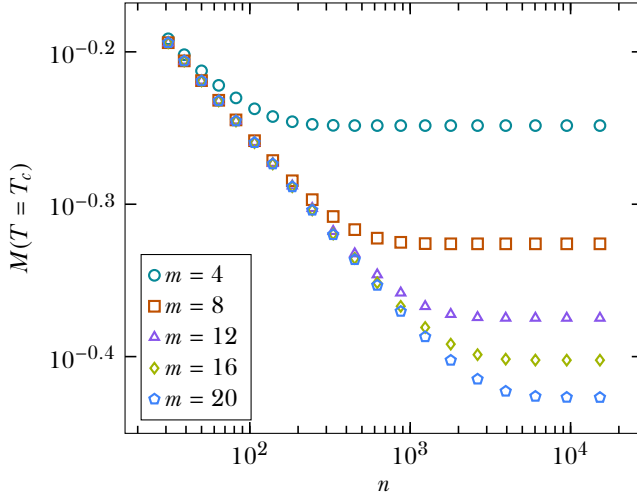


Figure 1.3: Behaviour of the order parameter at fixed m as function of the number of renormalization steps n . For small n , all curves coincide, since the system size is the only limiting length scale. For large enough n , the order parameter is only limited by the length scale $\xi(m)$. In between, there is a cross-over described by $\mathcal{G}(\xi(m)/N)$, given in Eq. 1.3.

1.1.2 Central charge

We may directly verify the value of the central charge c associated with the conformal field theory at the critical point by fitting to

$$S_{\text{classical}} \propto \frac{c}{6} \log \xi(m), \quad (1.5)$$

which yields $c = 0.501$, shown in the left panel of Fig. 1.4.

The right panel of Fig. 1.4 shows the fit to the scaling relation in N (or, equivalently the number of CTMRG steps n)

$$S_{\text{classical}} \propto \frac{c}{6} \log N, \quad (1.6)$$

which yields $c = 0.499$.

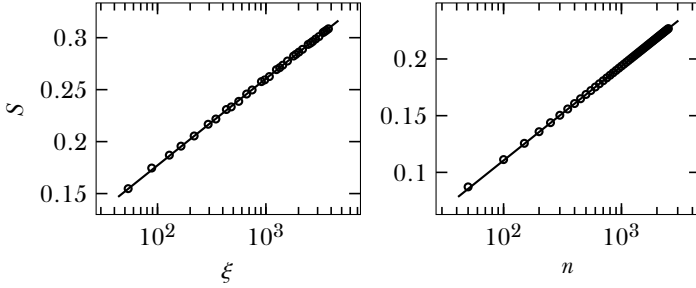


Figure 1.4: Left panel: numerical fit to Eq. 1.5, yielding $c = 0.501$. Here, $m \in \{8, 10, \dots, 70\}$ and the convergence threshold $\epsilon = 10^{-9}$. Right panel: numerical fit to Eq. 1.6, yielding $c = 0.499$, with the fit made to $n \in \{1500, 1550, \dots, 2500\}$, such that the truncation error is smaller than 10^{-7} .

1.1.3 Using the entropy to define the correlation length

Via ??, the correlation length is expressed as

$$\xi \propto \exp\left(\frac{6}{c}S\right). \quad (1.7)$$

Fig. 1.5 shows the results of fitting the relation in Eq. 1.1 with this definition of the correlation length. The fit is an order of magnitude better in the least-squares sense, and the half-moon shapes have almost disappeared, yielding a much more robust exponent of $\beta/\nu = 0.12498$.

The entropy uses all eigenvalues of the corner transfer matrix, making it apparently less prone to structure in the spectrum than the correlation length as defined in ??, which uses only two eigenvalues of the row-to-row transfer matrix. Furthermore, the corner transfer matrix \mathcal{A} is kept diagonal in the CTMRG algorithm, so S is much cheaper to compute than ξ .

1.1.4 Exponent κ

We now check the validity of the relation

$$\xi(m) \propto m^\kappa \quad (1.8)$$

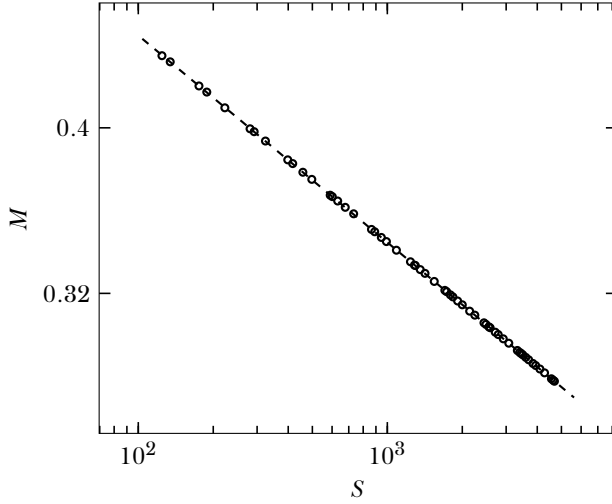


Figure 1.5: Fit to Eq. 1.1, using Eq. 1.7 as the definition of the correlation length. For the fit, we have used $m \in \{10, 11, \dots, 66\}$, calculated with convergence threshold $\epsilon = 10^{-9}$, yielding $\beta/\nu = 0.12498$.

in the context of the CTMRG method for two-dimensional classical systems. Similar checks were done for one-dimensional quantum systems in [2].

Let us first state that boundary conditions are relevant. From ?? we expect that for fixed boundary conditions, the entropy and therefore the correlation length is lower for a given bond dimension m .

There are various ways of extracting the exponent κ . Fig. 1.6 shows the results for fixed boundary conditions and Fig. 1.7 for free boundary conditions.

Directly checking Eq. 1.8 yields $\kappa = 1.93$ for a fixed boundary and $\kappa = 1.96$ for a free boundary.

Under the assumption of Eq. 1.8, we have the following scaling laws at the

critical point

$$M(m) \propto m^{-\beta \kappa / \nu} \quad (1.9)$$

$$f(m) - f_{\text{exact}} \propto m^{(2-\alpha)\kappa/\nu} \quad (1.10)$$

for the order parameter and the singular part of the free energy, respectively. With a fixed boundary, a fit to $M(m)$ yields $\kappa = 1.93$. For a free boundary we cannot extract any exponent, since $M = 0$ for every temperature. A fit to $f(m) - f_{\text{exact}}$ yields $\kappa = 1.90$ for a fixed boundary and $\kappa = 1.93$ for a free boundary. Fig. 1.6. Here, we have used $\beta = 1/8$, $\nu = 1$ and $\alpha = 0$ for the Ising model.

We may use ?? and ?? to check the relation

$$S_{\text{classical}} \propto \frac{c\kappa}{6} \log m, \quad (1.11)$$

which yields $\kappa = 1.93$ for a fixed boundary and $\kappa = 1.96$ for a free boundary, with $c = 1/2$ for the Ising model.

1.1.4.1 Comparison with exact result in asymptotic limit

The predicted value for κ [3] is $2.034 \dots$ (see also ??). With the CTMRG method, we extract the slightly lower value of 1.96 (corresponding to free boundary conditions). But, the structure in the quantities as function of m makes it hard to get an accurate fit to κ .

It is interesting to note that for fixed boundary conditions, the relation in Eq. 1.8 holds, but with a lower exponent κ . This is to be expected, since half the spectrum of the corner transfer matrix is missing.

1.2 Locating the critical point

In general, the critical point is not known, but it may be located by extrapolating the position of the pseudocritical temperature at finite system sizes.

The pseudocritical point can be defined in a variety of ways. In this chapter, we will define the pseudocritical point as the point of maximum entropy, as described in ?. Fig. 1.8 shows the classical analogue to the entanglement entropy as a function of temperature for different values of m .

The critical point is located by fitting the scaling law in ?.

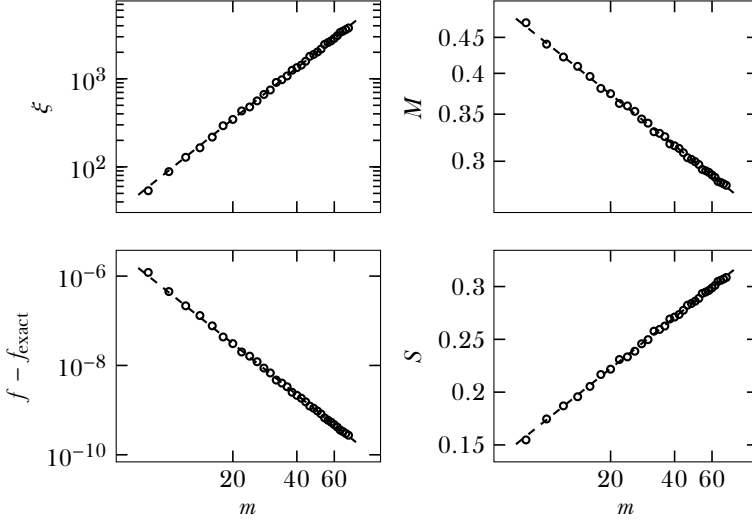


Figure 1.6: Numerical evidence for Eq. 1.8, Eq. 1.9, Eq. 1.11 with fixed boundary, yielding, from left to right and top to bottom, $\kappa = \{1.93, 1.93, 1.90, 1.93\}$. These values have been calculated from simulations with $m \in \{8, 10, \dots, 70\}$ and convergence threshold $\epsilon = 10^{-9}$.

1.2.1 Finite m

For approximations with finite bond dimension m , we may use different length scales to fit the scaling behaviour of $T^*(m)$. In light of the discussion in ??, we can choose either $\xi(T_c, m)$ or $\xi(T^*(m), m)$. The latter suffers less from finite-size effects, but is dependent on the accuracy with which T^* is located. It is, of course, of more general interest since T_c is normally not known.

Furthermore, we will consider both $\xi(m)$ derived from the row-to-row transfer matrix (??) and derived from the entanglement entropy (Eq. 1.7).

Fig. 1.9 shows the fits for different choices of this length scale. The results are tabulated in Table 1.1. To obtain T^* , we have calculated $T^*(m)$ for $m \in \{10, 11, \dots, 60\}$ with a convergence threshold of 10^{-8} and a temperature tolerance of 10^{-8} . The boundaries are fixed to +1.

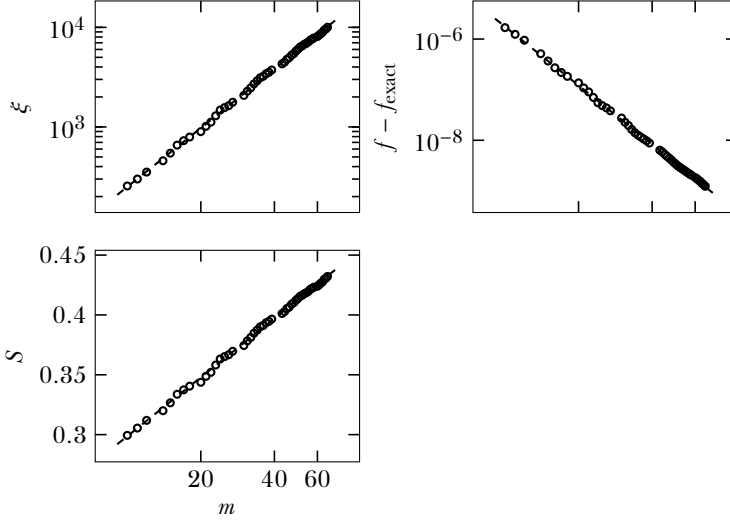


Figure 1.7: Numerical evidence for Eq. 1.8 with free boundary, yielding from left to right and then bottom $\kappa = \{1.96, 1.93, 1.96\}$. These values have been calculated from simulations with $m \in \{10, 11, \dots, 66\}$, but with $m \in \{13, 19, 28, 29, 40, 41, 42, 59\}$ left out, because for those values m the system breaks its symmetry (see ??). The convergence threshold was chosen to be $\epsilon = 10^{-7}$. It is not feasible to choose a lower threshold since more values of m break symmetry as machine precision is approached.

We denote the estimated value of the critical temperature as \widetilde{T}_c . Recall that the exact value is

$$T_c = 2.2691853 \dots \quad (1.12)$$

and

$$\nu = 1. \quad (1.13)$$

When using $\xi(T_c, m)$, the correlation length at the exact critical point, the result shows a lot of structure, yielding $\widetilde{T}_c = 2.269172$ and $\nu = 1.057$.

N_{eff}	T_c	ν
$\xi(T_c, m)$	2.269172	1.057
$\xi(T^\star(m))$	2.269183	1.002
$\exp((6/c)S(T^\star(m)))$	2.269183	1.02
m^κ	2.269181	–
N	2.269185	0.98

Table 1.1: Results for fits to the scaling law ?? using different length scales. When using m^κ , $\kappa \approx 1.91$ was found to give the best fit.

If, instead, the correlation length at the estimated pseudocritical temperature $\xi(T^\star(m))$ is used, the data shows less structure and we obtain the much more precise results $\tilde{T}_c = 2.269183$ and $\nu = 1.002$.

Another option is to use the entropy to define the correlation length, via [Eq. 1.7](#), which gave more accurate results than using the transfer matrix definition in [section 1.1.3](#). In this case, the results are slightly worse than the transfer matrix definition: $T_c = 2.269183$ and $\nu = 1.02$.

Finally, we may directly fit the law

$$|T_c - T^\star(m)| \propto m^{-\kappa/\nu}, \quad (1.14)$$

yielding $T_c = 2.269181$ and $\kappa/\nu = 1.91$. Incidentally, this is another way to confirm $\kappa \approx 1.9$ for systems with a fixed boundary.

1.2.2 Finite N

As a cross check, we can instead use systems of finite size to extract T_c and ν . We have calculated $T^\star(n)$ for $n \in \{2300, 2500, \dots, 7900\}$, with m big enough such that the truncation error is no larger than 10^{-6} . This yields $T_c = 2.269185$ and $\nu = 0.98$.

1.3 Away from the critical point

We may also verify the validity of the different length scales by asserting that the data for different values of m should collapse on a single curve

$$\mathcal{G}(t\xi(m)^{1/\nu}) = M(T, m)\xi(m)^{\beta/\nu}. \quad (1.15)$$

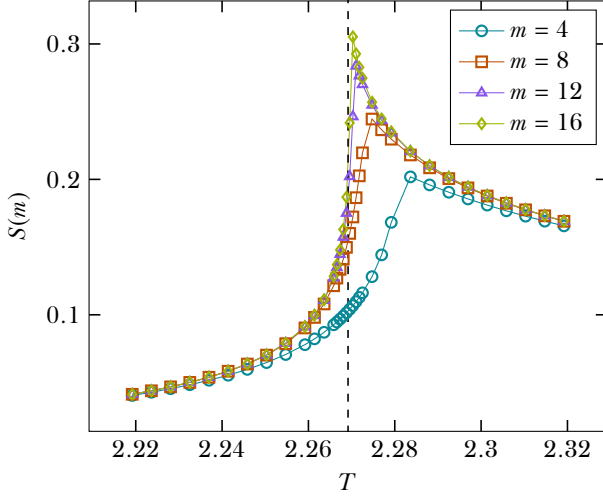


Figure 1.8: Classical analogue to the entanglement entropy, as in ??, near the critical point (shown as dashed line).

All data points were calculated with a convergence threshold of 10^{-7} . The values of the pseudocritical temperatures are taken from the results in [section 1.2](#). No temperatures beyond T_c is considered because the order parameter drops off sharply, causing the curve $\mathcal{G}(x)$ to tend to zero almost vertically, making the fitness P unreliable.

[Fig. 1.10](#) shows that for all length scales, the results more or less fall on one curve. [Table 1.2](#) shows the fitness of the data collapse [\[4\]](#) (given by ??) for all length scales used.

Using m^κ as a length scale for optimized fitness $P(\kappa)$ yields $\kappa \approx 1.98$, substantially higher than found previously for fixed boundary conditions.

As a cross-check, the bottom-right panel of [Fig. 1.10](#) shows data points for finite- N simulations. Here, the bond dimension is chosen such that the truncation error is smaller than 10^{-6} .

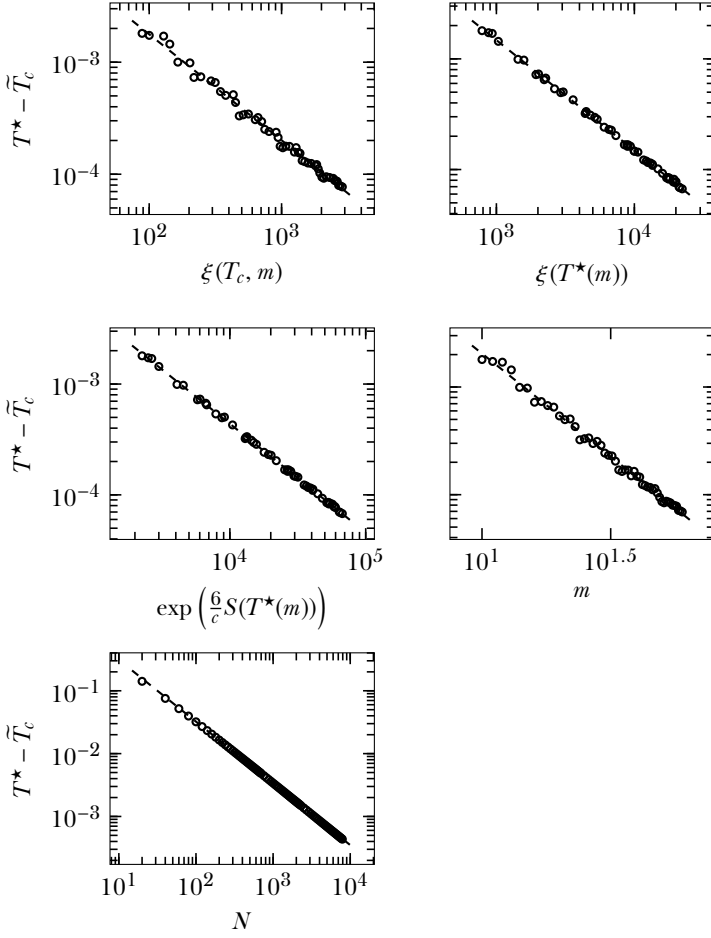


Figure 1.9: Fits to the scaling law $T^* - \tilde{T}_c \sim \xi(T_c, m)^\nu$. Results for the critical temperature and exponent ν are tabulated in [Table 1.1](#).

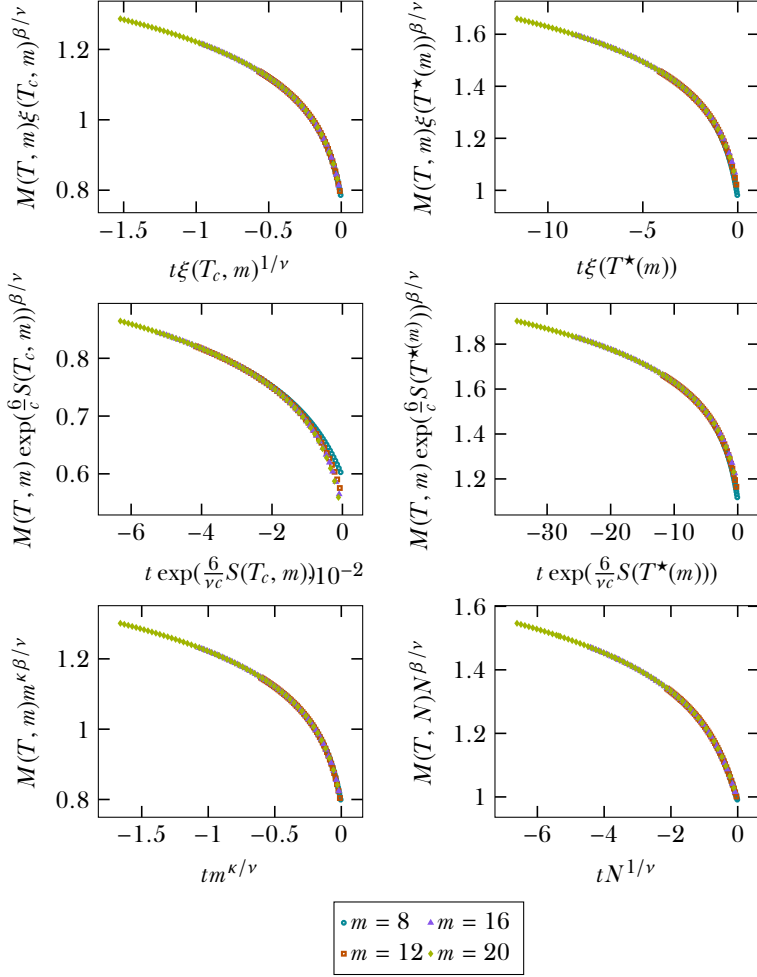


Figure 1.10: Data collapses using different length scales. For the bottom-right plot, approximations with finite N instead of finite m have been used, with $n = \{160, 480, 1000, 1500\}$ ($n = \frac{N-1}{2}$ is the number of algorithm steps).

N_{eff}	fitness P
$\xi(T_c, m)$	0.0075
$\xi(T^*(m))$	0.066
$\exp((6/c)S(T_c, m))$	0.057
$\exp((6/c)S(T^*(m)))$	0.087
m^κ	0.0080
N	0.0075

Table 1.2: Fitness of data collapse (??) for different length scales. $\kappa \approx 1.98$ was found to be optimal for the length scale m^κ .

1.4 Discussion

1.4.1 Finite- m vs finite-size simulations

With finite- m simulations, larger system sizes are accessible. This is clearly seen from the fact that for modest values of m , $T^*(m)$ is already closer to the critical point than $T^*(N)$ for the largest values of N .

For the Ising model, finite-size and finite- m scaling give comparable results. However, finite-size data is of much higher quality than the finite- m data, since the latter suffers from structure due to the spectrum of the corner transfer matrix, even when defining the correlation via the entanglement entropy. Therefore, it is likely that finite-size results improve significantly if correction to scaling terms are included in the fits.

For finite-size simulations, it is not entirely clear how the chosen bond dimension (and correspondingly, the truncation error) influences the precision of quantities and the position of the pseudocritical point. This could be analysed more thoroughly. A start with this has been made in ??.

It might be possible to simulate larger system sizes without much loss of accuracy, but it seems unlikely that the same system sizes as in the finite- m regime are accessible.

For finite- m results it is much easier to assess the convergence of quantities (see ??). The quality of the fit remains limited by the structure that is inherent in the data.

1.4.2 Exponent κ

We consistently find a value for the exponent κ that is between 1.93 and 1.96 (for simulations with free boundary conditions), while the theoretically predicted value is approximately 2.034.

The first reason for this might simply be the fact that the data has half-moon shaped patterns that make it hard to extract an exponent reliably.

A second possibility is that, since the predicted value for κ is only valid in the limit $m \rightarrow \infty$, finite- m effects cause the exponent obtained from numerical simulation to be lower. This is confirmed by the authors of [3], who use the iTEBD algorithm [5] to obtain $\kappa = 1.92$ for the Ising model and $\kappa = 1.26$ for the XXZ model (predicted value 1.34 . . .), among other results. However, the authors of [2] consistently find $\kappa \approx 2$ for the Ising model using iTEBD.

A third possibility is that the corner transfer matrices used for the calculations in this work do not represent optimal matrix-product states. In theory, the CTMRG algorithm should produce an optimized row-to-row transfer matrix with matrix product structure in the thermodynamic limit [6]. But because simulations with free boundary conditions are sensitive to numerical errors, we could only choose a moderately low convergence threshold. This might in part explain the observed discrepancy.

Bibliography

- ¹T. Nishino, K. Okunishi, and M. Kikuchi, “Numerical renormalization group at criticality”, *Physics Letters A* **213**, 69–72 (1996).
- ²L. Tagliacozzo, T. R. De Oliveira, S. Iblisdir, and J. I. Latorre, “Scaling of entanglement support for matrix product states”, *Physical Review B* **78**, 024410 (2008).
- ³F. Pollmann, S. Mukerjee, A. M. Turner, and J. E. Moore, “Theory of finite-entanglement scaling at one-dimensional quantum critical points”, *Physical Review Letters* **102**, 255701 (2009).
- ⁴S. M. Bhattacharjee, and F. Seno, “A measure of data collapse for scaling”, *Journal of Physics A: Mathematical and General* **34**, 6375 (2001).
- ⁵G. Vidal, “Classical simulation of infinite-size quantum lattice systems in one spatial dimension”, *Physical Review Letters* **98**, 070201 (2007).
- ⁶R. J. Baxter, *Exactly solved models in statistical mechanics* (Elsevier, 1982) Chap. 13.